



# Synthesis and Electrochemical Properties of a New Molybdenum (VI) Complex with Schiff Base Ligand

Madhavi Devi. D

Asst Professor, Dept of Chemistry, DIET, Hyderabad (India)

## ABSTRACT

The reaction of 2-pyridylamino-N,N-bis(2-methylene-4,6-bitert-butylphenol) (H<sub>2</sub>L') and MoCl<sub>5</sub> gives a molybdenum (VI) complex [MoL'(O)<sub>2</sub>] 1, which has been characterized by single-crystal X-ray diffraction, IR and NMR analysis. Electrochemical studies show that 1 can electrocatalyze hydrogen evolution, both from acetic acid with a turnover frequency (TOF) of 36.4 moles of hydrogen per mole of pre-catalyst per hour at an overpotential of 441.6 mV (in DMF), and from buffer (pH 7.0) with a TOF of 373.1 moles of hydrogen per mole of catalyst per hour at an overpotential of 787.6 mV.

**Keywords:** Molybdenum (VI) complex, X-ray molecular structure, Molecular electrocatalysts, Hydrogen evolution

## I. INTRODUCTION

Hydrogen is one of the most ideal energy in the future, because of its potential to reduce the current dependence on fossil fuels [1]. Effective proton reduction to form H<sub>2</sub> has been a subject of intense study and significant effort has been made to design metal complexes for proton reduction [2,3]. In Nature, hydrogenase enzymes [4,5] can efficiently catalyze both the production and oxidation of hydrogen using earth-abundant metals (nickel and iron). However, enzymes are difficult to adapt for commercial applications and their stability is often limited outside of their native environment [6,7]. Electrolysis of water is the simplest way to produce hydrogen. To increase the reaction rate and lower the overpotential, it is necessary to use an efficient hydrogen evolution reaction (HER) electrocatalyst. Many research groups, including ours, have focused on the development of molecular catalysts employing the more abundant metals, and several complexes that contain nickel [8,9], cobalt [10-12], copper [13,14] and molybdenum have been developed as electrocatalysts for the reduction of water to form H<sub>2</sub> [15-18]. A report from Chang and co-workers described a highly active molecular molybdenum(IV) electrocatalyst, [(Py5Me<sub>2</sub>)MoIVO]<sub>2</sub><sup>+</sup> (Py5Me<sub>2</sub>=2,6-bis(1,1-bis(2-pyridyl)ethyl)pyridine, a neutral pentadentate ligand) that reduces water to H<sub>2</sub> at neutral pH in aqueous buffer, reporting a maximum of 1,600 moles of H<sub>2</sub> per mole of catalyst per hour at an overpotential of 642 mV [15]. To investigate the roles of the oxidation/reduction site in molybdenum complexes, determining of their redox potentials and characterization of their electronic structures, we focus our work in the design and catalytic properties of molybdenum (VI) complexes. We have previously shown that the molybdenum (VI) complexes supported by 2-pyridylamino-N,N-bis-phenol (**Figure 1**) also can be molecular electrocatalysts for hydrogen evolution [16-18]. It has been shown that the donor type and electronic properties of the ligands play vital roles in determining the structure and reactivity of the corresponding metal complexes. With this mind, we chose 2-pyridylamino-N,N-bis(2-methylene-4,6-bitert-butylphenol) (H<sub>2</sub>L'), a potential deprotonated ligand to react with MoCl<sub>5</sub> to assembly the

corresponding molybdenum compound and study its electrocatalytic function. Here we present the synthesis, structure, characterization and properties of a new molybdenum (VI) electrocatalyst,  $[\text{MoL}'(\text{O}_2)]$  1, as well as the effect of tetradentate ligand modifications on the catalytic properties of molybdenum (VI) complexes.

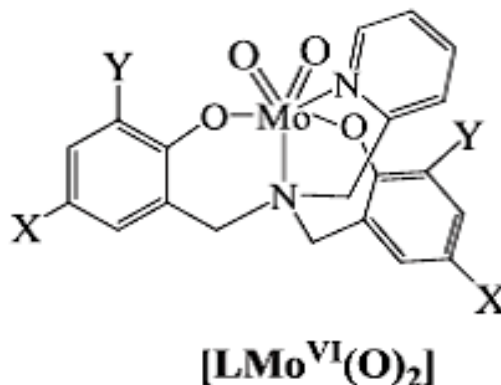


**Figure 1: Structures of a series of molybdenum(VI) complexes,  $[\text{LMo}(\text{O})_2]$  ( $\text{X}=\text{Y}=\text{F}$ ) and  $[\text{LMo}(\text{O})_2]$  ( $\text{X}=-\text{OMe}$ ,  $\text{Y}=-\text{t-Bu}$ ).**

## II. MATERIALS AND METHODS

### 2.1 Physical measurements

$^1\text{H}$  NMR spectra were measured on a Bruker AM 500 spectrometer in  $\text{CDCl}_3$ . Infrared spectra were obtained with a Bruker FTIR 1730 infrared spectrometer. Cyclic voltammograms were obtained on a CHI-660E electrochemical analyzer under oxygen-free conditions using a three-electrode cell in which a glassy carbon electrode, 1 mm in diameter) was the working electrode, a saturated  $\text{Ag}/\text{AgNO}_3$  or  $\text{Ag}/\text{AgCl}$  electrode was the reference electrode, and a platinum wire was the auxiliary electrode. In organic media, the ferrocene/ferrocenium (1+) couple was used as internal standard and 0.10 M  $[(\text{n-Bu})_4\text{N}]\text{ClO}_4$  was used as the supporting electrolyte. Controlled-potential electrolysis (CPE) in DMF was conducted using an air-tight glass double compartment cell separated by a glass frit. The working compartment was fitted with a glassy carbon plate and an  $\text{Ag}/\text{AgNO}_3$  reference electrode. The auxiliary compartment was fitted with a Pt gauze electrode. The working compartment was filled with 50 mL of 0.4 mM acetic acid in a 0.10 M  $[(\text{n-Bu})_4\text{N}]\text{ClO}_4$  DMF solution, while the auxiliary compartment was filled with 35 mL of 0.10 M  $[(\text{n-Bu})_4\text{N}]\text{ClO}_4$  DMF solution, resulting in equal solution levels in both compartments. Both compartments were sparged for 60 min with  $\text{N}_2$  and cyclic voltammograms were recorded as controls. CPE in aqueous media was also conducted using an air tight glass double compartment cell separated by a glass frit. The working compartment was fitted with a glassy carbon plate and an  $\text{Ag}/\text{AgCl}$  reference electrode. The auxiliary compartment was fitted with a Pt gauze electrode. The working compartment was filled with 50 mL of 0.25 M phosphate buffer solution, while the auxiliary compartment was filled with 35 mL phosphate buffer. Both compartments were sparged for 60 min with  $\text{N}_2$  and cyclic voltammograms were recorded as controls. After addition of complex 1, cyclic voltammograms were recorded. After electrolysis, a 0.5 mL aliquot of the headspace was removed and replaced with 0.5 mL of  $\text{CH}_4$ . The headspace sample was injected into the gas chromatograph (GC). GC experiments were carried out with an Agilent Technologies 7890A gas chromatography instrument (Column: 19091J-413,



No. USC184265H; Detector: TCD; Injection volume: 1 mL). Synthesis of 2-pyridylamino-N,N-bis(2-methylene-4,6-bitert-butylphenol), H<sub>2</sub>[O<sub>2</sub>NN]BuEtPy (H<sub>2</sub>L')

A solution of 2,4-bibutylphenol (30.95 g, 0.123 mol), aminomethylpyridine (8.11 g, 0.061 mol), and 37% aqueous formaldehyde (9.17 mL, 0.123 mol) in water (50 mL) was stirred and refluxed for 8 h. Upon cooling, a large quantity of beige solid formed. The solvents were decanted, and the remaining solid residue was washed with cold methanol to give a pure, white powder (29.60 g, 93.4% yield). Crystalline product was obtained by slow cooling of a hot diethyl ether solution. Anal. calcd for C<sub>32</sub>H<sub>44</sub>N<sub>2</sub>O<sub>2</sub>: C, 78.58; H, 9.00; N, 5.73%. Found C, 78.33; H, 8.88; N, 5.81%. <sup>1</sup>H NMR {400 MHz, CDCl<sub>3</sub>} δ 10.55 (2H), 8.73 (1H), 7.72 (1H), 7.30 (2H), 7.26 (1H), 7.16 (1H), 6.96 (2H), 3.86 (6H), 1.43 (18H), 1.32 (18H).

### 2.3 Synthesis of complex 1

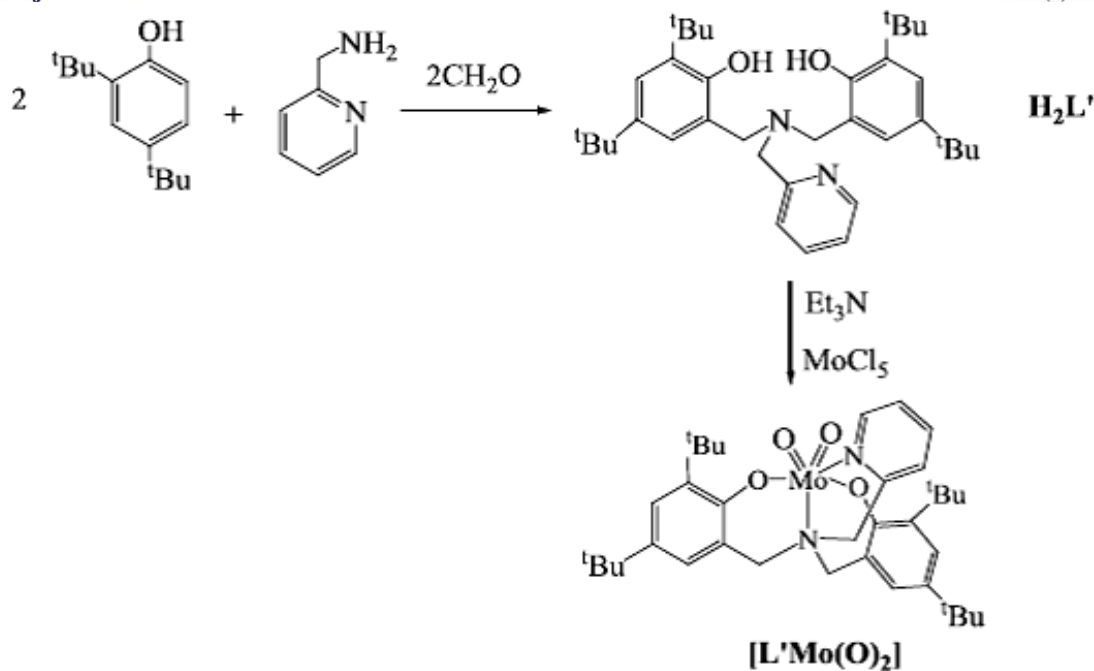
To a solution, containing H<sub>2</sub>L' (0.516 g, 1 mmol) and triethylamine (0.10 g, 1 mmol) in methanol (20 ml), MoCl<sub>5</sub> (0.273 g, 1 mmol) was added and the mixture was stirred for 15 min. Single crystals were obtained from the filtrate which was allowed to stand at room temperature for several days, collected by filtration, and dried in vacuo (65%). The elemental analysis results (Found C, 62.67; H, 6.67; N, 4.71. C<sub>32</sub>H<sub>42</sub>N<sub>2</sub>O<sub>4</sub>Mo requires C, 62.31; H, 6.87; N, 4.54) were in agreement with the formula of the sample used for X-ray analysis. <sup>1</sup>H NMR {400 MHz, CDCl<sub>3</sub>} δ 9.12 (1H), 7.49 (1H), 7.12 (3H), 6.92 (2H), 6.73 (1H), 4.99 (2H), 3.96 (2H), 3.74 (2H), 1.26 (36H). IR (cm<sup>-1</sup>): 931 and 905 (νMo=O).

### 2.4 Crystal structure determination

The X-ray analysis of 1 was carried out with a Bruker SMART CCD area detector using graphite monochromated Mo-K $\alpha$  radiation ( $\lambda=0.71073$  Å) at room temperature. All empirical absorption corrections were applied using the SADABS program [19]. The structure was solved using direct methods and the corresponding non hydrogen atoms were refined anisotropically. All the hydrogen atoms of the ligands were placed in calculated positions with fixed isotropic thermal parameters and included in the structure factor calculations in the final stage of full-matrix least-squares refinement. All calculations were performed using the SHELXTL computer program [20]. CCDC 1032589 contains the supplementary crystallographic data for this paper. The data can be obtained free of charge from The Cambridge Crystallographic Data Centre [21]. Crystallographic data for complex 1 are given in **Table S1** and selected bond lengths are listed in **Table S2**.

## III. RESULTS AND DISCUSSION

In the presence of Et<sub>3</sub>N, the reaction of H<sub>2</sub>L' (**Figure S1**) with MoCl<sub>5</sub> affords the molybdenum (VI), [MoL'(O<sub>2</sub>)] 1 in 65% yield (**Scheme 1**), which is in agreement with the result of NMR analysis (**Figure S2**). The IR spectrum of complex 1 displays two strong νMo=O bands at 931 cm<sup>-1</sup> and 905 cm<sup>-1</sup> (**Figure S3**), characteristic for symmetric and asymmetric vibrational modes, respectively, of the cis-[MoO<sub>2</sub>]<sup>2+</sup> fragment [22,23].



**Scheme 1: Schematic representation of the synthesis of [L'Mo(O)<sub>2</sub>].**

Complex 1 crystallizes in space group P-1, with one unit present per unit cell. As shown in **Figure 2**, the X-ray structure of complex 1 reveals a six-coordinate Mo atom in a distorted octahedral coordination geometry, with fac coordination of the ligand. The molybdenum oxo groups show the expected mutual cis configuration. The Mo=O bond lengths [Mo1-O2, 1.697(3) Å; Mo1-O5, 1.705(4) Å] are in the expected range for cis-dioxo MoVI complexes [16-18,24,25]. The Mo–O bond lengths [1.952(3) Å and 1.960(3) Å] are shorter than those observed in other Mo (VI) complexes [26,27]. The Mo–N bond lengths fall in the range of 2.369(4) Å to 2.372(4) Å, and are comparable to those observed in a similar Mo (VI) complex [26].

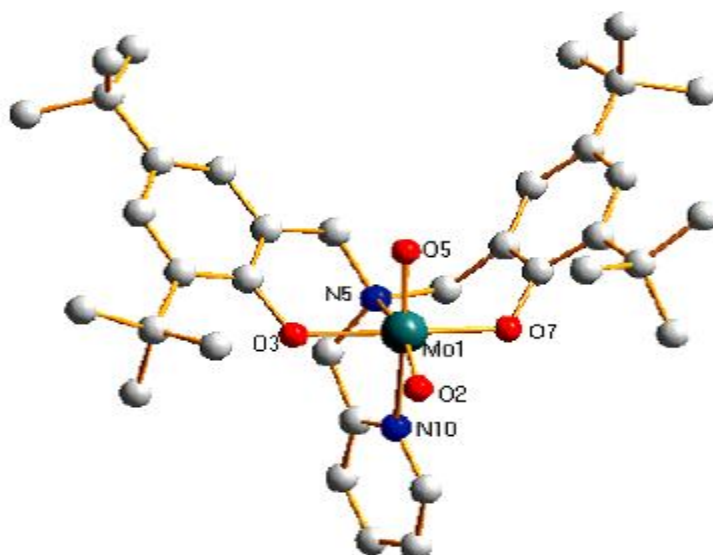


**Figure 2: Antimicrobial activity of substituted 2-benzylidene-1,3-indandiones.**

In **Figure 3a**, the cyclic voltammogram of complex 1 shows one quasi-reversible redox couple at -1.23 V and one reversible couple at -1.77 V versus Fc<sup>+</sup>/Fc, which can be assigned to the couples of MoVI/V [28] and

MoV/IV, respectively. As observed in **Figure S4**, the current response of the redox event at -1.84 V shows linear dependence on the square root of the scan rate, indicative of a diffusion controlled process, with the electrochemically active species freely diffusing in the solution. To determine the possible electrocatalytic activity of complex 1, cyclic voltammograms were recorded in the presence of acetic acid. **Figure 3b** shows a systematic increase in *i<sub>cat</sub>* observed near -1.84 V with increasing acid concentration from 0.0 mM to 4.0 mM. This rise in current can be attributed to the catalytic generation of H<sub>2</sub> from acetic acid [15], with the catalytic onset shifted to more positive potentials (from -1.24 V to -0.95 V). Based on the above observations, we postulate the catalytic cycle depicted in **Scheme 2** for the generation of hydrogen from acetic acid mediated by complex 1. Two-electron reduction of [MoVIL'(O)<sub>2</sub>] gives [MoIVL'(O)] and releases one O<sub>2</sub><sup>-</sup> ion. Addition of proton produces the reactive intermediate [MVIL'(OH)(H)]. Then affords H<sub>2</sub> and gives rise to a cycle in which [MoVIL'(O)] precedes the formation of [MoVIL'(O)<sub>2</sub>] 1. More detailed mechanistic studies are under investigation.

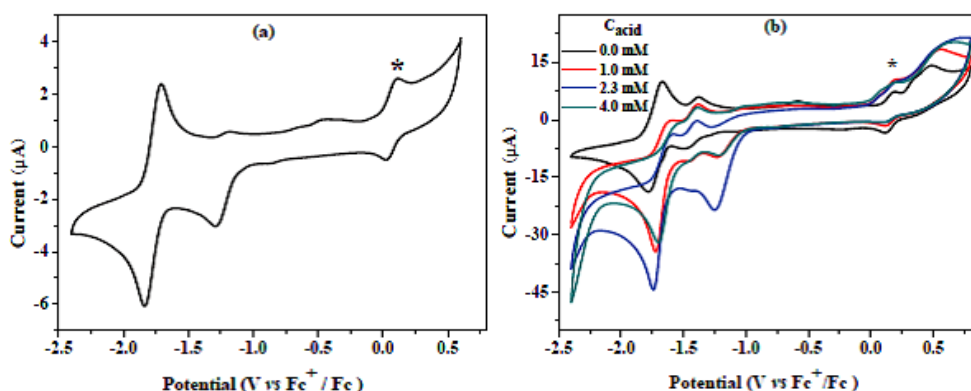
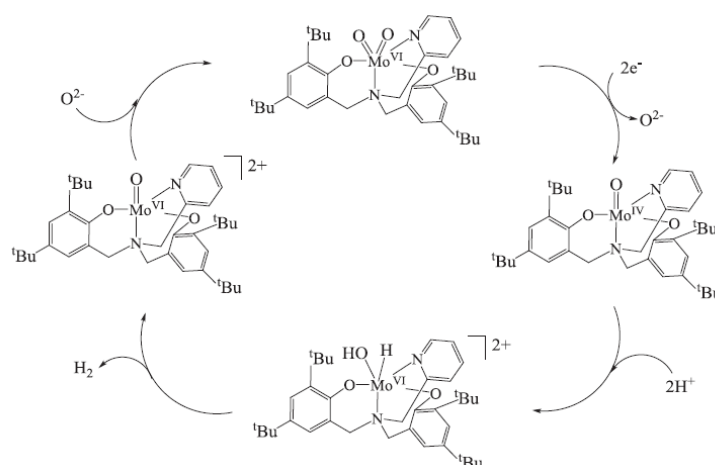


**Figure 3:** a) Cyclic voltammogram of complex 1 in DMF. b) Cyclic voltammograms of a 1.56 mM solution of complex 1, with varying concentrations of acetic acid in DMF. Conditions: 0.10 M [n-Bu<sub>4</sub>N]ClO<sub>4</sub> as supporting electrolyte; scan rate: 100 mV/s; glassy carbon working electrode (1 mm diameter); Pt counter electrode; Ag/AgNO<sub>3</sub> reference electrode; Fc internal standard (\*).



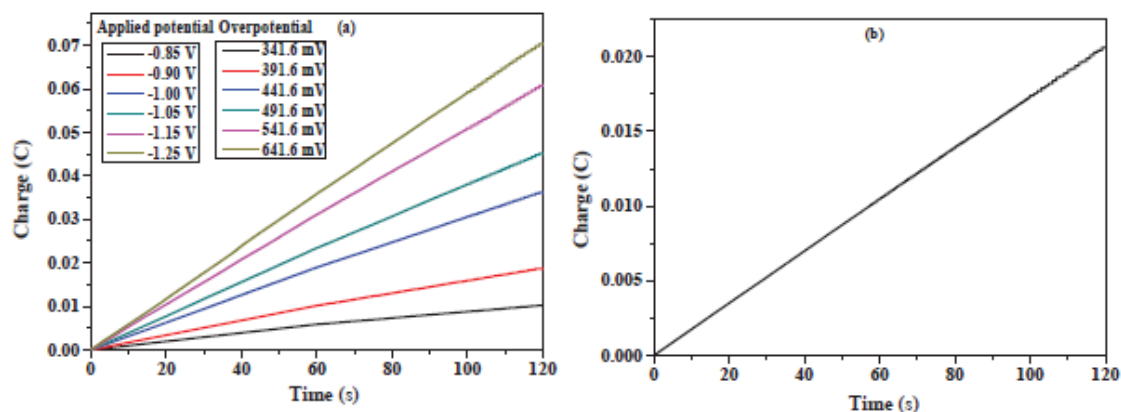
**Scheme 2:** The possible catalytic mechanism for proton reduction by catalyst 1.

Further evidence for the electrocatalytic activity of complex 1 was obtained by bulk electrolysis of a DMF solution of the complex (0.16 μM) with acetic acid (4.0 mM) at variable applied potential using a glassy carbon

plate electrode in a double compartment cell. **Figure 4a** exhibits the total charge for bulk electrolysis of complex 1 in the presence min of electrolysis, accompanying evolution of a gas, which was confirmed as H<sub>2</sub> by gas chromatography. According to **Figure S5**, ~31.5 μL of H<sub>2</sub> was produced over an electrolysis period of 1 h. The CPE experiment under the same potential with a catalyst-free solution only gave a charge of 20 mC (**Figure 4b**), showing that this complex does indeed serve as an effective hydrogen production catalyst under such conditions. Assuming every catalyst molecule was distributed only on the electrode surface and every electron was used for the reduction of protons, according to Eq. 1 and 2 [17,29], we calculated the TOF for the catalyst as reaching a maximum of 36.4 moles of hydrogen per mole of catalyst per hour at an overpotential of 441.6 mV (Eq. S1 and **Figure S6**), which is similar to that of [L<sub>2</sub>MoVI(O)<sub>2</sub>] (L=2-pyridylamino-N,N-bis(2-methylene-4-methoxy-6-tert-butylphenol) ion) (39 moles of hydrogen per mole of catalyst per hour at an overpotential of 441.6 mV), a similar type of complex [18], and is much lower than that of [L<sub>2</sub>MoVI(O)<sub>2</sub>] (L=2-pyridylamino-N,N-bis(2-methylene-4,6-difluorophenol) ion) (50.6 moles of hydrogen per mole of catalyst per hour at an overpotential of 441.6 mV) [17]. The result is consistent with an evident increase in the catalytic activity when electron-withdrawing groups are present at the phenol para-position of the ligand, and 2-pyridylamino- N,N-bis(2-methylene-4,6-difluorophenol) constitutes the better active catalyst [30].

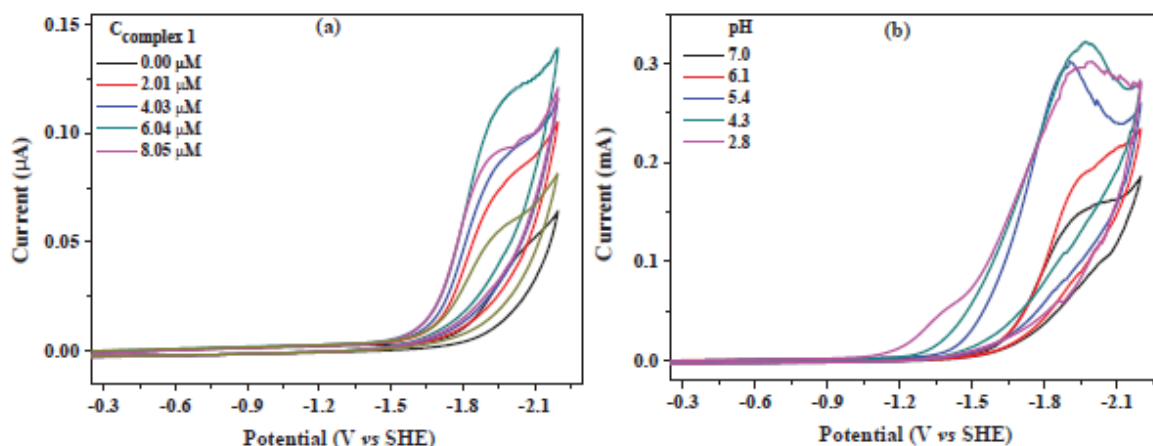
$$\text{TOF} = \Delta C / (F \times n_1 \times n_2 \times t) \quad (1)$$

Overpotential=Applied potential-E<sup>⊙</sup>HA=Applied potential-(E<sup>⊙</sup>H<sup>+</sup>-(2.303RT/F)pK<sub>a</sub>HA) (2) where ΔC is the charge from the catalyst solution during CPE minus the charge from the solution without catalyst during CPE, F is Faraday's constant, n<sub>1</sub> is the moles of electrons required to generate one mol of H<sub>2</sub>, n<sub>2</sub> is the moles of catalyst in solution, and t is the duration of electrolysis.



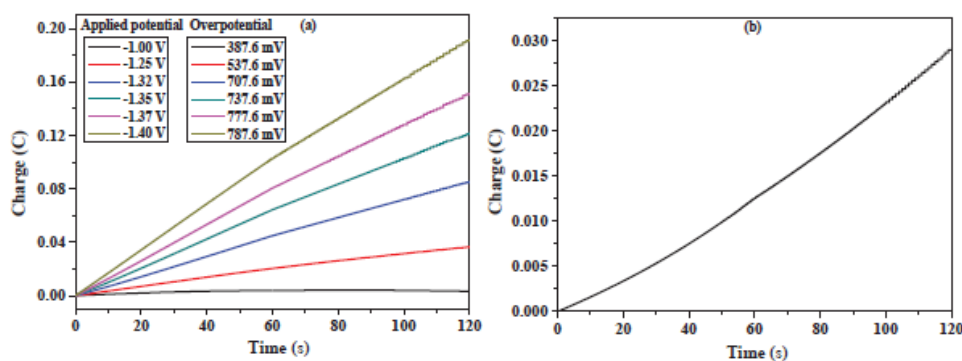
**Figure 4:** a) Charge buildup versus time from electrolysis of a 0.10 M [Bu<sub>4</sub>N]ClO<sub>4</sub> solution with 0.16 μM complex 1 in DMF under various applied potentials. All data have been deducted blank. b) Charge buildup versus time from electrolysis of a 0.10 M [Bu<sub>4</sub>N]ClO<sub>4</sub> solution in DMF under -1.25 V vs Ag/AgNO<sub>3</sub>.

To explore the catalytic hydrogen evolution in aqueous media, CVs were conducted in 0.25 M phosphate buffers at different pH values. As shown in **Figure 5a**, in the absence of complex 1, the catalytic current was not apparent until a potential of -1.55 V versus SHE was attained. With addition of complex 1, the onset of catalytic current was observed at about -1.30 V versus SHE, and the current strength increased significantly with increasing concentrations of complex 1 from 0.00 μM to 8.05 μM. Furthermore, it was found that the catalytic onset was also dependent on pH value of buffer (**Figure 5b**).



**Figure 5:** a) Cyclic voltammograms of complex 1 at various concentrations. b) CVs of complex 1, showing the variation in catalytic current with pHs.

Catalytic hydrogen production can also be achieved with complex 1 in buffer, **Figure 6a** shows the total charge of bulk electrolysis of the solution containing 0.08  $\mu\text{M}$  complex 1 at pH 7.0. When the applied potential was -1.40 V versus Ag/AgCl, the maximum charge was only 29 mC during 2 min of electrolysis in absence of complex 1 (**Figure 6b**). Under the same conditions, the charge reached 192 mC with addition of complex 1 (0.08  $\mu\text{M}$ ), accompanying gas bubble appeared. The evolved H<sub>2</sub> was analyzed by gas chromatography, **Figure S7**, which gave  $\sim 0.37$  mL of H<sub>2</sub> over an electrolysis period of 1 h with a Faradaic efficiency of 93% for H<sub>2</sub> (**Figure S8**). The CPE under the same conditions without complex 1 only gave  $\sim 0.12$  mL of H<sub>2</sub> over an electrolysis period of 1 h (**Figure S9**), showing that this complex does indeed can catalyze hydrogen evolution. According to Eq. 1 and 3 [11,15], we calculated the TOF for the catalyst as reaching a maximum of 373.1 moles of hydrogen per mole of catalyst per hour at an overpotential of 787.6 mV (Eq. S2 and **Figure S10**), where

$$\text{Overpotential} = \text{Applied potential} - E(\text{pH}) = \text{Applied potential} - (-0.059 \text{ pH})$$


**Figure 6:** a) Charge build up versus time from electrolysis of a 0.25 M buffer (pH 7.0) with 0.08  $\mu\text{M}$  complex 1 under various applied potentials. All data have been deducted blank. b) Charge build-up versus time from electrolysis of a 0.25 M buffer (pH 7.0) under -1.40 V vs Ag/AgCl.

This value is much lower than that of [(Py5Me<sub>2</sub>)MoIVO]<sub>2</sub><sup>+</sup> [15], indicating that the molybdenum(IV) electrocatalyst is more active than the molybdenum (VI) species.



In summary, we have successfully prepared a new molybdenum (VI) complex 1, which can generate dihydrogen from acetic acid or water. Our ongoing efforts are focused on modifying the Schiff base ligands to give related water-soluble complexes for further functional studies, with an emphasis on chemistry relevant to sustainable energy cycles.

## REFERENCES

- [1] Lewis NS, Nocera DG (2006) Powering the planet: chemical challenges in solar energy utilization. *Proc Nat Acad Sci* 103: 15729-15735.
- [2] McKone JR, Marinescu SC, Brunschwig BS, Winkler JR, Gray HB (2014) Earth-abundant hydrogen evolution electrocatalysts. *Chem Sci* 5: 865-878.
- [3] Vincent KA, Parkin A, Armstrong FA (2007) Investigating and exploiting the electrocatalytic properties of hydrogenases. *Chem Rev* 107: 4366-4413.
- [4] Fontecilla-Camps JC, Volbeda A, Cavazza C, Nicolet Y (2007) Structure/function relationships of [NiFe]- and [FeFe]- hydrogenases. *Chem Rev* 107: 4273-4303.
- [5] Vignais PM, Billoud B (2007) Occurrence, classification, and biological function of hydrogenases: an overview. *Chem Rev* 107: 4206-4272.
- [6] Pickett CJ, Tard C (2009) Structural and functional analogues of the active sites of the [Fe]-, [NiFe]-, and [FeFe]-hydrogenases. *Chem Rev* 109: 2245-2274.
- [7] Darensbourg MY, Wegand W (2011) Sulf-oxygenation of Active Site Models of [NiFe]- and [FeFe]-Hydrogenases; Commentary on Chemical Models of Hydrogenase Enzyme Oxygen Sensitivity Possibilities. *Eur J Inorg Chem* 2011: 994- 1004.